

Magnetism of quantum dot clusters: A Hubbard model study

J.-P. Nikkarila^{1,2}, M. Koskinen¹ and M. Manninen¹

¹*NanoScience Center, Department of Physics, FIN-40014 University of Jyväskylä, Finland and*

²*Inspecta LTD, FI-02151 Espoo, Finland*

(Dated: April 30, 2008)

Magnetic properties of two and three-dimensional clusters of quantum dots are studied with exact diagonalization of a generalized Hubbard model. We study the weak coupling limit, where the electrons interact only within a quantum dot and consider cases where the second or third harmonic oscillator shell is partially filled. The results show that in the case of half-filled shell the magnetism is determined by the antiferromagnetic Heisenberg model with spin 1/2, 1 or 3/2, depending on the number of electrons in the open shell. For other fillings the system in most cases favors a large total spin, indicating a ferromagnetic coupling between the dots.

PACS numbers: 73.21.La, 75.75.+a, 71.10.-w

I. INTRODUCTION

Experiments have shown that cluster structure can show stronger form of magnetism than the bulk structure of the same element. This interesting behavior has been reported for example for Fe, Ni and Co clusters^{1,2,3,4,5}. The size of clusters in these experiments has varied from few to few hundreds of atoms. Also Ga has been shown to exhibit paramagnetic behavior with many cluster sizes⁴. The experiments have started an intensive theoretical epoch in material physics, where for example the Ising model⁶, the Hubbard model^{7,8}, and different forms of the Density Functional Theory (DFT), are applied^{9,10,11,12}.

Experimental breakthroughs have also been achieved in constructing artificial lattices from quantum dots^{13,14,15}. The artificial quantum dot molecules and normal molecules (or clusters) have many differences, where the most important one is that the geometrical structure of an artificial molecule is fixed and the degeneracy can not be removed by Jahn-Teller deformation. This gives room for internal symmetry breaking through spontaneous magnetism, superconductivity or superfluidity. Recent experiments have inspired much theoretical work^{16,17,18,19,20,21,22,23,24,25,26,27}.

For a lattice with strongly correlated particles the generic many-particle model is the Hubbard model, which has been vastly studied in the case of one state per lattice site (for reviews see^{28,29}). In a one-dimensional lattice or in a ring the Hubbard model is exactly solvable using the Bethe ansatz³⁰. The magnetism of finite molecules^{7,8} and quantum rings^{31,32} have also been studied using the simple Hubbard model.

Mean-field calculations based on the spin-density functional theory, as well as ab initio configuration interaction calculations, predict that the Hund's first rule determines the total spin of an isolated quantum dot, independent of the interparticle interaction and confining potential of the lattice site^{9,10,33}. The magnetism of the quantum dot molecule then depends on the total spin of the individual dots, on the geometry of the molecule and on the coupling between the quantum dots^{34,35,36,37,38}. A simple tight-binding model (with the exchange splitting as a

parameter) explains qualitatively some of the magnetic properties of quantum dot lattices³⁹.

Single quantum dots with a few electrons can be solved numerically exactly (i.e. to a high degree of convergence with respect to the necessary restrictions in Hilbert space) by diagonalizing the many-body Hamiltonian (for a review see Ref.¹⁰). Methods beyond the mean-field approximation have also been applied to quantum dot molecules^{40,41,42,43,44,45}.

The purpose of this paper is to study the magnetism of quantum dot molecules with a generalized Hubbard model. We consider dot molecules with two to four dots in two and three-dimensional geometries and up to 12 electrons per dot. We assume the confining potential in each dot to be two-dimensional or three dimensional and harmonic at the bottom. In this case the electrons in one dot fill the harmonic oscillator shells. We consider the three lowest shells $1s$, $1p$, and $2s1d$. We use a generalization of the simple Hubbard model to describe the interactions: The particles interact only within a quantum dot and only the partially filled shell is included in the Hilbert space. The Hubbard Hamiltonian is then solved with exact diagonalization.

II. THEORETICAL MODELS

A. General Hubbard model

We assume a generalized Hubbard model Hamiltonian

$$\hat{H} = \hat{J} + \hat{U}, \quad (1)$$

where the first term represents hopping between neighboring sites and the second term intra-site two-body interactions.

Hoppings preserve spin, and are equal for spin-up and spin-down particles. Thus, \hat{J} separates into two symmetric spin parts: $\hat{J} = \sum_{\sigma=\uparrow,\downarrow} \hat{J}_{\sigma}$. The hopping part of the Hamiltonian is generally of the form

$$\hat{J}_{\sigma} = - \sum_{nn'} \sum_{jj'} J_{nn'jj'} c_{nj\sigma}^{\dagger} c_{n'j'\sigma}, \quad (2)$$

where n and n' refer to different dots, whereas j and j' denote the orbitals in question, in n and n' , respectively. In the case of p and d orbitals we consider directional dependence of the hopping integrals J (see below). In the case of a square shaped four-dot molecule we assume that there is no diagonal hopping.

The two-body interactions of the Hubbard model are treated in the spirit of the tight-binding model: The electrons only interact when they are at the same quantum dot. Thus, \hat{U} separates in the symmetric parts representing interactions on each site n : $\hat{U} = \sum_n \hat{U}_n$. Within a site, full (spin-independent) two-body interaction is considered, which yields

$$\hat{U}_n = \frac{1}{2} \sum_{\substack{j_1 j_2 j_3 j_4 \\ \sigma \sigma'}} U_{j_1 j_2 j_3 j_4} c_{n j_1 \sigma}^\dagger c_{n j_2 \sigma'}^\dagger c_{n j_4 \sigma'} c_{n j_3 \sigma} \quad (3)$$

where $U_{j_1 j_2 j_3 j_4}$ are the direct space matrix elements of on-site interaction, depending on the interaction itself and the j -orbitals in question, i.e. the eigenstates of the confining potential.

We do not take advantage of the fact that the Hamiltonian does not depend on spin, but diagonalize the system for $S_z = 0$ for even number of electrons and for $S_z = 1/2$ for odd number of electrons and only afterwards determine the total spin S for each many-particle state. The total number of electrons is denoted by N . Lanczos method was used to diagonalize the matrix. The largest matrix dimensions, for four dot systems with 12 electrons, were more than 800000 with more than 1.5 billion nonzero elements.

B. On-site interactions

We consider mainly two-dimensional systems and two kinds of interactions between the electrons, the delta function interaction and the Coulomb interaction. In the case of the delta function interaction and harmonic confinement, the relative ratios of the matrix elements $U_{j_1 j_2 j_3 j_4}$ (Eq. (3)), for each electron shell k , can be characterized by just one constant U_k . Furthermore, for the p -shell the ratio of the two different matrix elements is independent of the radial form of the confining potential. In the case of the Coulomb interaction we have determined the interaction matrix elements only for the harmonic confinement. We consider only the open shell in each dot to be in the active Hilbert space and only need the interaction matrix elements in each shell separately. These are given in Table I. Notice that for the p -shell the only difference in going from the short-range delta function interaction to the long-range Coulomb interaction is the reduction of one U value as compared to the others.

For triangular and tetrahedral clusters of quantum dots we consider also three-dimensional dots. This we do only within the p -shell where the nonzero matrix elements are the same as in the two-dimensional case, but now also including the p_z -orbitals.

TABLE I: Nonzero interaction matrix elements for each energy shells of a two-dimensional harmonic confinement calculated with the delta function interaction (U^δ) and with the Coulomb interaction (U^C). U_k determines the strength of the contact interaction. In the case of the Coulomb interaction the matrix elements are given in atomic units for harmonic potential with eigenfrequency $\omega_0 = 1$ atomic units. For p -electrons we show for the delta function interaction the matrix elements for two representations: For p_x and p_y and for the angular momentum states p_- and p_+ .

shell	j_1	j_2	j_3	j_4	$U_{j_1 j_2 j_3 j_4}^\delta$	$U_{j_1 j_2 j_3 j_4}^C$
1	s	s	s	s	U_1	1.2533
2	p_x	p_x	p_x	p_x	$3U_2$	
2	p_x	p_x	p_y	p_y	U_2	
2	p_x	p_y	p_x	p_y	U_2	
2	p_x	p_y	p_y	p_x	U_2	
2	p_y	p_y	p_y	p_y	$3U_2$	
2	p_-	p_-	p_-	p_-	$2U_2$	0.86160
2	p_-	p_+	p_-	p_+	$2U_2$	0.86160
2	p_-	p_+	p_+	p_-	$2U_2$	0.23494
2	p_+	p_+	p_+	p_+	$2U_2$	0.86160
3	$2s$	$2s$	$2s$	$2s$	$4U_3$	0.74901
3	$2s$	$2s$	$1d_+$	$1d_-$	$2U_3$	0.13949
3	$2s$	$1d_+$	$2s$	$1d_-$	$2U_3$	0.66823
3	$2s$	$1d_+$	$1d_+$	$2s$	$2U_3$	0.13949
3	$2s$	$1d_-$	$2s$	$1d_-$	$2U_3$	0.66823
3	$2s$	$1d_-$	$1d_-$	$2s$	$2U_3$	0.13949
3	$1d_+$	$1d_+$	$1d_+$	$1d_+$	$3U_3$	0.71595
3	$1d_+$	$1d_-$	$1d_+$	$1d_-$	$3U_3$	0.71595
3	$1d_+$	$1d_-$	$1d_-$	$1d_+$	$3U_3$	0.12846
3	$1d_-$	$1d_-$	$1d_-$	$1d_-$	$3U_3$	0.71595

C. Hopping parameters

In the simple Hubbard model with one state per site the hopping is between two s -states and independent of the direction. In the case of higher angular momentum states we have to consider also directional dependence. We have done this for the p -electrons and d -electrons.

The (unnormalized) wave functions of the two-dimensional harmonic confinement are

$$\begin{aligned} \langle \mathbf{r} | 1s \rangle &= e^{-\alpha r^2} \\ \langle \mathbf{r} | p_\pm \rangle &= r e^{-\alpha r^2} e^{\pm i\phi}, \quad \left(\text{or } \langle \mathbf{r} | p_\xi \rangle = \xi e^{-\alpha r^2} \right), \\ \langle \mathbf{r} | 2s \rangle &= (2\alpha r^2 - 1) e^{-\alpha r^2}, \\ \langle \mathbf{r} | d_\pm \rangle &= r^2 e^{-\alpha r^2} e^{\pm 2i\phi}, \end{aligned} \quad (4)$$

where α depends on the oscillator parameter of the confinement, ξ is either x or y , and $r = \sqrt{x^2 + y^2}$. For p -electrons we use both angular momentum presentation and Cartesian coordinates. Naturally the results are independent of the choice of the coordinate system. We use the Cartesian coordinates for studying three-dimensional

dots with p -electrons. In that case $r = \sqrt{x^2 + y^2 + z^2}$ and ξ can also be z .

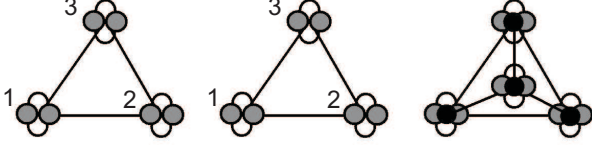


FIG. 1: Schematic picture of triangular and tetrahedral clusters considered. Left: triangle with p_x and p_y orbitals; center: triangle with p_x , p_y and p_z orbitals; right: tetrahedron with p_x , p_y and p_z orbitals.

Figure 1 shows triangular and tetrahedral clusters with p -orbitals. At the vertices electrons can occupy states p_x , p_y (and also p_z in 3D cases). We assume that the hopping probability is proportional to the overlap of the wave functions at neighboring sites. The overlap integral depends on the factor $t = \alpha R^2$, where R is the distance between the sites. Each nonzero overlap is proportional to factor

$$A = \frac{32}{\alpha} e^{-\alpha R^2/2} = \frac{32}{\alpha} e^{-t/2} \quad (5)$$

Some of the overlap integrals are zero due to the symmetry. The overlap integrals of the p_z -electrons for a triangle and tetrahedron are given in Table II. In the case of four dots in a square the hopping between neighboring dots is along x or y direction and in this case the hopping from p_x to p_y is not possible. In the case of angular momentum representation the hopping probability also depends on the direction due the phases of the wave functions. Table III gives the hopping parameters in x and y directions for the p and sd shells. Note that the hopping probability is of the same order between all the states.

We have only one parameter t describing the hopping probability. Notice, however, that the ratios of the different hopping parameters depend on t , i.e. on the distance between the dots. In real systems the parameter t and the on-site interactions U are coupled. However, we keep them as independent parameters in order to get a more general picture of the possible magnetic structures. In realistic systems where the tight-binding model (and thus the Hubbard model) is expected to be valid, the parameter t should be of the order of 10 or larger. It turns out, however, that already when $t \gtrsim 4$ the results are qualitatively independent of t .

D. Heisenberg model

It is well-known that in the limit of large U/t the simple Hubbard model with one s -state per site approaches the antiferromagnetic Heisenberg model. We will study if the clusters with half filled p or sd shells will also give the same spectrum as the Heisenberg model. The effective

TABLE II: Hopping parameters $J_{nn'jj'}$ (in units of A) for j and j' orbitals (p_x , p_y and p_z orbitals) at vertices n and n' of a triangle and a tetrahedron. The symbol n_1 refers to triangle's vertices 1 and 2 (see Fig. 1), whereas symbols n_2 and n_3 go through all 1, 2 and 3 ($n_2 \neq n_3$). The table for tetrahedron shows the additional hopping parameters from the triangle to the fourth vertex. In the case of two signs, the upper sign is for $n_1 = 1$ and the lower sign for $n_1 = 2$.

Triangle					Tetrahedron				
n	n'	j	j'	$J_{nn'jj'}/A$	n	n'	j	j'	$J_{nn'jj'}/A$
1	2	p_x	p_x	$(1-t)$	n_1	4	p_x	p_x	$(1-t/4)$
1	2	p_y	p_y	1	n_1	4	p_y	p_y	$(1-t/12)$
1	2	p_x	p_y	0	n_1	4	p_x	p_y	$\mp t/4\sqrt{3}$
n_1	3	p_x	p_x	$(1-t/4)$	n_1	4	p_x	p_z	$\mp t/\sqrt{6}$
n_1	3	p_y	p_y	$(1-3t/4)$	n_1	4	p_y	p_z	$-t/3\sqrt{2}$
n_1	3	p_x	p_y	$\mp t\sqrt{3}/4$	n_1	4	p_z	p_z	$(1-2t/3)$
n_2	n_3	p_x	p_z	0	3	4	p_x	p_x	1
n_2	n_3	p_y	p_z	0	3	4	p_y	p_y	$(1-t/3)$
n_2	n_3	p_z	p_z	1	3	4	p_x	p_y	0
					3	4	p_x	p_z	0
					3	4	p_y	p_z	$\sqrt{2}t/3$
					3	4	p_z	p_z	$(1-2t/3)$

TABLE III: Hopping parameters for the p shell and sd shell calculated for the angular momentum states. $J_{nn'jj'}^{\text{as}}$ gives the asymptotic ratios ($t \rightarrow \infty$) of the hopping parameters (note that even though $t \rightarrow \infty$, $J_{nn'jj'} \rightarrow 0$ due to the prefactor A). The hopping direction is along x and y axis. In the case of two signs, the upper sign is for hopping to x -direction and the lower sign to y -direction.

j	j'	$J_{jj'}/A$	$J_{nn'jj'}^{\text{as}}/A$
p_+	p_+	$-(t-2)/2$	$-t/2$
p_+	p_-	$\mp t/2$	$\mp t/2$
$2s$	$2s$	$(-2+t)^2/4$	t
$2s$	d_+	$\pm t(-4+t)/4\sqrt{2}$	$\pm t/\sqrt{2}$
d_+	d_+	$(8-8t+t^2)/8$	$t/2$
d_+	d_-	$t^2/8$	$t/2$

Heisenberg Hamiltonian is

$$\hat{H}_{\text{eff}} = \frac{1}{2} J_{\text{eff}} \sum_{n \neq n'}^L \mathbf{S}_n \cdot \mathbf{S}_{n'} + \text{constant}, \quad (6)$$

where L is the number of dots and J_{eff} is the effective coupling which depends on the hopping parameters and the on-site interaction. The spin depends on the number of electrons in each dot and is determined by the Hund's first rule. In the half-filled case the spin is $1/2$, 1 , and $3/2$ for the $1s$, $1p$ and $2s1d$ shells, respectively. Note that in most cases of the clusters considered here the Heisenberg model is exactly solvable^{32,46}.

III. RESULTS

A. Quantum dot Dimer

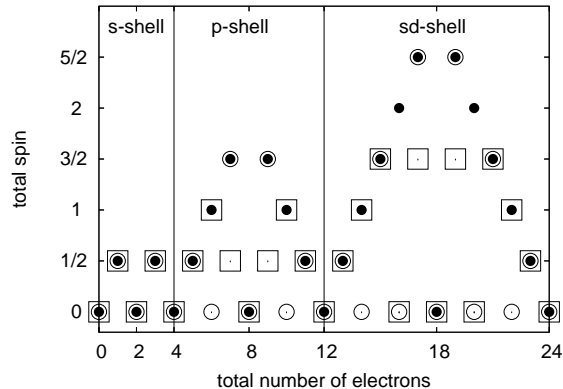


FIG. 2: Total spin as a function of the number of electrons in a quantum dot dimer. The solid dots are the results for the lateral and vertical dimer with delta function interaction. The open circles and squares are the results for Coulomb interaction for lateral and vertical dimer, respectively. In all cases the ratio of the largest U and largest J is $U_{\max}/J_{\max} = 10$.

We first consider two weakly connected quantum dots. Figure 2 shows the total spin as a function of electrons in the quantum dot dimer. In the case of the full shells, $N = 4, 12, 24$, the spin is naturally zero. In the case of half filled shells the spin is also zero. However, in that case each dot has the spin determined by the Hund's rule, but the spins are opposite as in an antiferromagnet. This was confirmed by looking at the conditional probability.

Figure 2 shows results for two lateral dots where the dots are in the same plane and for two vertical dots where the dots are on top of each other. In the lateral case the hopping probabilities are those given in Table III while in the vertical case the symmetry allows hopping is only between same orbitals in both dots. In the case of the delta function interaction the total spin is the same for lateral and vertical configurations.

In general, for an open shell quantum dot the Hund's rule determines the spin¹⁰. This is the case whatever is the the interactions between the particles, as long as it is repulsive. In the case of the delta function interaction the favored magnetic coupling between the two dots is ferromagnetic. Only the half-filled case is antiferromagnetic. In the case of the long-range Coulomb interaction the situation is more complicated: There is a delicate competition between the ferromagnetic and antiferromagnetic coupling, and the total spin can also be between the largest possible and zero, as seen in Fig. 2.

The antiferromagnetic order of the half-filled shell can be seen also by looking at the energy spectrum of the

lowest state. The Heisenberg Hamiltonian, Eq. (6), for two spins gives energies $\epsilon(S) = S(S+1)J_{\text{eff}}$, where S is the spin of the state which gets values $0, 1, \dots, S_{\max}$. Denoting by K_S the ratio $K_S = (\epsilon(S) - \epsilon(0)) / (\epsilon(1) - \epsilon(0))$ we notice that for the Heisenberg model $K_S = S(S+1)/2$. These ratios can now be compared to those determined from energy spectrum of the Hubbard model.

TABLE IV: Ratios of energy differences K_S of half-filled double dots compared to those of the Heisenberg model. The last column gives the ratio of the largest on-site energy to the largest hopping integral.

Shell	System	Interaction	K_1	K_2	K_3	U_{\max}/J_{\max}
Heisenberg			1	3	6	
p	lateral	delta	1	3.06		30.0
p	lateral	Coulomb	1	3.20		10.0
p	vertical	delta	1	2.98		10.0
p	vertical	Coulomb	1	2.68		30.0
sd	lateral	delta	1	3.01	6.03	40.0
sd	lateral	Coulomb	1	3.01	6.04	75.0
sd	lateral	Coulomb	1	3.44	11.93	7.5
sd	vertical	delta	1	3.00	5.79	40.0
sd	vertical	Coulomb	1	2.93	5.71	15.0

Table IV shows the calculated energy ratios for different two dot molecules with half-filled p or sd shells. The results show a good agreement with the antiferromagnetic Heisenberg model. The results depend on the ratio of the on-site energies U and the hopping parameters J as indicated in the case of lateral Coulomb system. The larger is the ratio U_{\max}/J_{\max} the better the Heisenberg model describes the lowest energy states.

In the case of the Coulomb interaction the spin is zero for all even numbers of electrons. Each dot then has an integer number of electrons and its spin is determined by the Hund's rule. The conditional probability shows that the coupling between the dots is antiferromagnetic. This result is in agreement with that of the local spin density approximation³⁸.

B. Triangle of quantum dots with with p orbitals

Next we study the magnetic properties of trimers, where the quantum dots form vertices of an equilateral triangle as shown in Fig. 1. We considered two cases: Two-dimensional quantum dots, where only the p_x and p_y orbitals in each dot can be occupied and a three-dimensional case, where each dot is spherically symmetric having also the p_z orbital. In the case of the triangle we only used the onsite matrix elements calculated with the delta function interaction.

Figures 3 and 4 show results of the 2D case. In the case of the half-filled orbital one would expect antiferromagnetic coupling. Indeed, the total spin of the ground state is zero for $N = 6$. In the case of the triangle the antiferro-

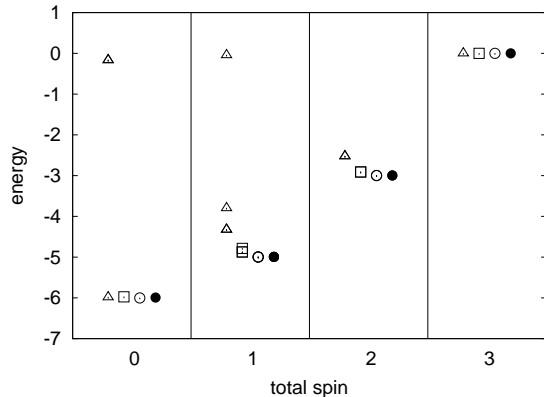


FIG. 3: Lowest energy levels of the Hubbard model for a triangle (without p_z electrons) with half-filled p -shell compared with the results of the antiferromagnetic Heisenberg model with spin $S = 1$. The distance between the dots R is 3 (triangles), 3.5 (squares), 4 (circles) and 5 (dots). In all cases $\alpha = 1$ and $U_2 = 1$. The results for $R = 5$ agree exactly with those of the Heisenberg model. The energies have been scaled so that the ground state energy is -6.

magnet is frustrated. The conditional probability is then not very helpful for confirming the antiferromagnetism. However, in the case of a triangle the antiferromagnetic Heisenberg Hamiltonian can be solved exactly and the energy spectrum can be compared to that of the Hubbard model. This is done in Fig. 3 for different values of the interdot distance, i.e hopping probability. The figure shows that all the results are in agreement with those of the Heisenberg model, which becomes more accurate when the interdot distance increases. In the case of a triangle the Heisenberg model has only one energy state for each total spin with degeneracies 1, 2, 3, and 1 for $S = 0, 1, 2$, and 3, respectively.

Figure 4 shows the ground state spin as a function of the total number of electrons in the triangle for three different values of the hopping parameter. In the weak coupling limit (black dots) the spin is at maximum for $N > 6$, meaning ferromagnetic coupling between the dots. For less than half-filled case, $N < 6$, the situation is more complicated. The weak coupling limit (black dots) show maximum spin, except for $N = 5$ where $S = 3/2$ (instead of the largest possible $5/2$). When the coupling between the dots gets stronger, the total spin gets smaller and the tendency to ferromagnetism disappears. This is illustrated also in the energy plot in Fig. 4 where the energy difference between the $S = 0$ (or $S = 1/2$) and the maximum spin state is plotted for different values of the coupling. Weak coupling favors ferromagnetism except for the half-filled case while strong coupling favors small total spin.

We also computed the triangle of quantum dots including also the p_z orbitals orthogonal to the plane of

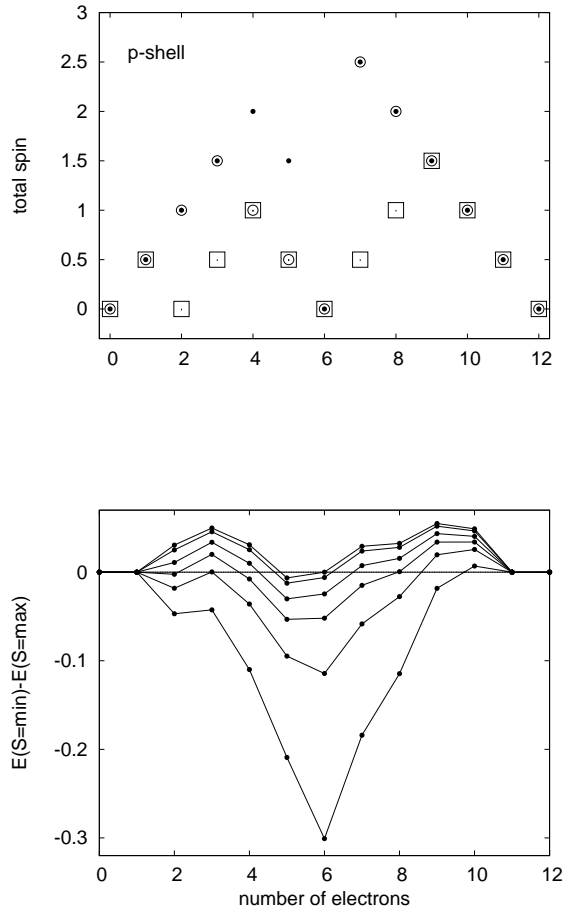


FIG. 4: Upper panel: Total spin as a function of the total number of p -electrons in a triangular cluster of quantum dots. The interdot distance R is 3 (squares), 3.5 (circles) and 4 (dots). $U_2 = 1$. Lower panel: Energy difference between the $S = 0$ (or $S = 1/2$) state and the polarized state with $S = N/2$ calculated for $U_2 = 1$ and for different values of the hopping parameter γJ , where J is determined with $R = 4$ and γ has values 0.01, 1, 4, 8, 16, 100 (from top to down).

the triangle. Naturally, in this case each dot can occupy 6 electrons and a half-filled dot will have spin $3/2$ due to Hund's rule. The triangle with half-filling ($N = 9$) had again low-energy spectrum in perfect agreement with the Heisenberg model for spin $3/2$. For other fillings the ferromagnetic order was favored in the weak coupling case, just like in the case of the triangle without the p_z orbitals. It is interesting to note that the antiferromagnetic Heisenberg model for half-filled case seems to be independent of how the coupling between the individual dots is made. For example, when the p_z orbitals are included in the weak coupling limit, the hopping between them is nearly prohibited and their role is just to increase the spin per dot, i.e. the spin of the Heisenberg model.

C. Tetrahedron with p_x and p_y and p_z orbitals on its vertices

The only three-dimensional cluster we considered is a tetrahedron. In this case we only studied the p shell and included all the three p -orbitals. We considered only the delta function interaction and used the Cartesian p -orbitals, the overlaps of which are given in Table II.

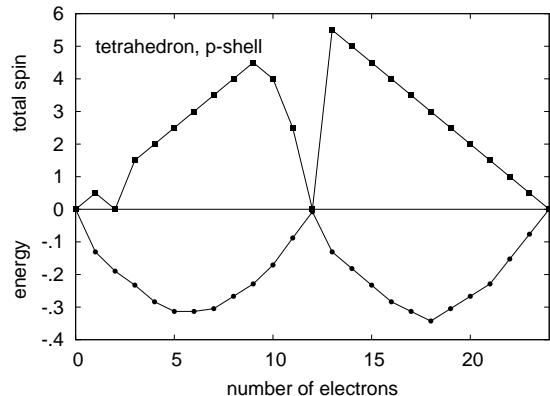


FIG. 5: Total spin and ground state energy of four quantum dots forming a tetrahedron, as a function of the total number of p -electrons (including p_z electrons). The distance between the dots is $R = 4$ and the $U_2 = 1$. Note that the energy for the antiferromagnetic ground state for $N = 12$ is not zero but $E = -.007533$.

The results show that for strong hopping (small distance between the dots) and weak interaction (small U_2) the total spin is mainly 0 or 1 indicating no magnetism. For large U_2 or weak coupling between the dots the results are closely related to those observed for a triangle. Figure 5 shows the total ground state energy and the total spin as a function of the number of electrons. The parameters correspond to the weak coupling limit. Like in the case of a triangle, the system is ferromagnetic for more than half-filling of the p shell ($N > 12$), while for less than half filling the spin is slightly reduced for some electron number. In exactly half-filled case the result is again a Heisenberg antiferromagnet with a very good accuracy.

The total energy plotted in Fig. 5 shows that it has minima at $N = 5$ and $N = 18$ corresponding roughly $1/4$ and $3/4$ fillings. Note that for $N > 12$ the energy shown is the ground state energy from which the average on-site repulsion, $U_2(N - 12)$, has been subtracted. In the half-filled case the energy is only slightly negative, arising from 'virtual' hopping between dots.

The asymmetry of the total spin (and energy) with respect of the half filling in the case of triangle and tetrahedron can be traced back to the single particle levels of the tight binding model in these systems: They are not

TABLE V: Total spin of the ground state for a four dot square and row and row with periodic boundary conditions (noted a Row+). N is the total number of p electrons in the four dot system. C refers to Coulomb interaction and δ to delta function interaction. $U_{\max}/J_{\max} = 17.2$ for Coulomb interaction and 20 for delta function interaction. In the cases of square with 2 and 14 electrons the ground state is degenerate with spins 0 and 1.

N	Square C	Square δ	Row δ	Row+ δ
2	0,1	0,1	0	1
4	0	2	2	0
6	0	0	3	3
8	0	0	0	0
10	0	0	3	3
12	0	2	2	0
14	0,1	0,1	0	1

symmetrically distributed around the zero energy.

D. Four dots in a square and in a row: The p -shell

In the case of a square the hopping parameters are easier to determine. In the case of p orbitals we have only hopping from p_x to p_x and from p_y to p_y as shown in the first two rows of the Table II for triangles. The hopping is more favorable when the orbitals point towards the neighboring dot. In the square this leads to an interesting situation where an electron, say in p_x orbital, can easily hop on the x -direction, but can not continue easily around the square since every second hop would be in the y -direction. The square is thus different from a row of four dots with periodic boundary conditions, as illustrated in Fig. 6. In the latter case the electron can continue through the row with easy hops.

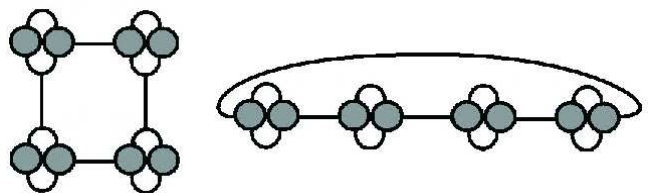


FIG. 6: Schematic picture illustrating the easy hops between p -electrons in a square and in a row with periodic boundary condition.

Table V shows the total spin of the ground state of the four dot square as a function of the filling of the p shell. The result is compared to that of the row of four dots and the row with periodic boundary conditions. In the case of the Coulomb interaction the total spin of the ground state of the square of quantum dots is zero for all (even) numbers of p -electrons. In the case of the delta function interaction the cases with $N = 4$ and $N = 12$ favor maximizing the spin. The row of four dots

favors ferromagnetism. It is interesting to note that the difference in the hopping probabilities between p_x and p_y orbitals seem to be important for the magnetic coupling between the dots. For example, for $N = 6$ and $N = 10$ the total spin is zero in the case of the square, while it has its maximum value in the case of a row with periodic boundary conditions.

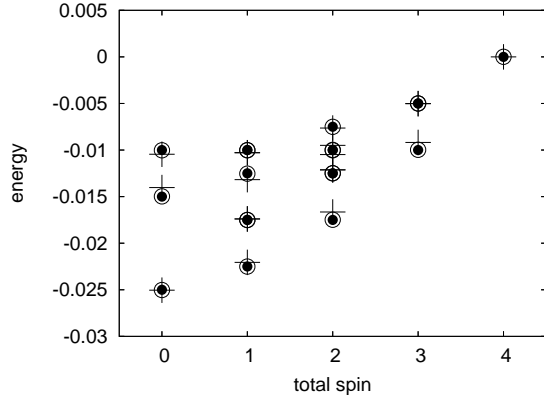


FIG. 7: Energy spectrum of a square of quantum dots with half-filled p -levels ($N=8$). Black dots: results of the antiferromagnetic Heisenberg model. Open circles: results of the Hubbard model with delta function interaction and $U_{\max}/J_{\max} = 40$. Plus-signs: results of the Hubbard model with Coulomb interaction and $U_{\max}/J_{\max} = 17.2$. The energies of the Heisenberg model and Coulomb interaction are scaled and shifted so that the lowest and highest energies shown agree with those of the Hubbard model with the delta function interaction.

In the half-filled case each system has zero total spin. Figure 7 shows the comparison of the lowest energy states of the half-filled case with those of the Heisenberg anti-ferromagnetic square with $S = 1$. For the delta function interaction the agreement is perfect. In the case of the long-range Coulomb interaction the quantitative agreement is not exact but qualitatively the spectra are still the same. It is important to note that the directional dependence of the hopping, i.e. the fact that the electron can not go easily around the square without exchanging the orbital from p_x to p_y , does not seem to have any effect on the validity of the Heisenberg model.

E. Four dots in a square and in a row: The sd -shell

In this section we consider four dot systems where in each dot the sd shell is partially filled. We assume the dots to be two-dimensional. The open shell then has $2s$, d_+ and d_- orbitals. The on-site interactions are given in Table I and the hopping integrals in Table III above. For simplicity we use only the asymptotic values of the

hopping parameters and, consequently, we have only one free parameter which is the ratio U_{\max}/J_{\max} .

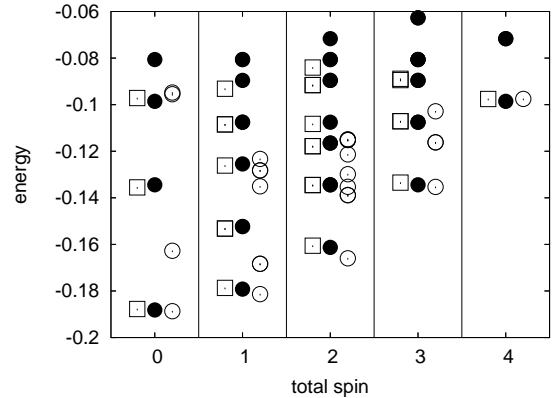


FIG. 8: 25 lowest energy states for 12 sd electrons in a square calculated with the delta function ($U_{\max}/J_{\max} = 10$), squares, and with the Coulomb interaction ($U_{\max}/J_{\max} = 7.5$), open circles, compared with the results of the Heisenberg model, black dots. The results for the Coulomb interaction and the Heisenberg model have been scaled and shifted so that the ground state and the lowest $S = 4$ state agree with those of the delta function interaction.

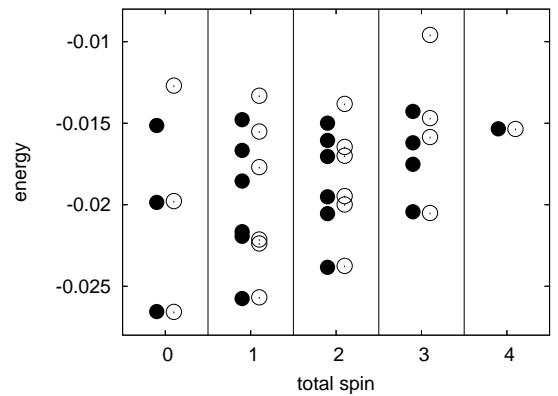


FIG. 9: 25 lowest energy states for 12 sd electrons in a row of four quantum dots. Black points are results for a row of vertical dots calculated with the delta function interaction ($U_{\max}/J_{\max} = 40$), open circles are results for a row of lateral dots calculated with the Coulomb interaction ($U_{\max}/J_{\max} = 7.5$). The results Coulomb interaction have been scaled and shifted so that the ground state and the lowest $S = 4$ state agree with those of the delta function interaction.

We first studied the ground state spin as a function of the total (even) number of electrons for a square of quantum dots using the Coulomb interaction. In the case

$N = 2$ and $N = 22$ electrons the ground state is degenerate with spins 0 and 1. For $N = 4$ the total spin of the ground state is 2 and for $N = 10$ it is 1. For all other even numbers of electrons the spin of the ground state is zero. In the case of a row of four lateral dots we studied the ground state only up to half filling. The total spin for the row is zero for $N = 2, 4, 6, 8$ and 12, but for $N = 10$ it is 3. Kolehmainen *et al*³⁸ studied the square of four quantum dots with 16 *sd*-electrons using the local spin density approximation. They found the ground state to be ferromagnetic which is in disagreement with the present result $S = 0$, suggesting that the LSDA can not describe correctly the strongly correlated system in this case.

In the case of half-filling, i.e. with $N = 12$, we compared the low energy spectra with that of the Heisenberg model with $S = 3/2$. Figure 8 shows the 25 lowest energy states for the square of four dots calculated with the Coulomb and delta function interactions, compared to the results of the Heisenberg model. The delta function interaction reproduces nearly perfectly the spectrum of the Heisenberg model. Note that more levels are shown for the Heisenberg model and that some of the levels are degenerate. In the spectrum of the Coulomb interaction the lowest state for each spin is still in fair agreement with the Heisenberg model, but the higher levels do not agree.

We also studied in detail the spectrum of half-filled row of four dots. In this case we do not have an analytic solution for the Heisenberg model. Instead we computed the row of four dots in the vertical arrangement using the delta function interaction and using a large ratio $U_{\max}/J_{\max} = 40$, which we believe gives nearly exactly the result of the Heisenberg model (for $S = 3/2$). Figure 9 shows a comparison of that result with the spectrum of a lateral row of four dots with Coulomb interaction. In this case the agreement of with the spectra is surprisingly good.

IV. CONCLUSIONS

We have studied the magnetism of the ground states of clusters of quantum dots. We described each quantum dot with a harmonic confinement and used a generalized Hubbard model for describing the interaction between the dots. For the on-site interaction we used either the Coulomb interaction or the delta function interaction. Only the partially filled harmonic oscillator shell was used as an active basis of the many-particle calculation.

The quantum dot dimer favors ferromagnetic ground state when the interaction is short range delta function. Only the half-filled shells have antiferromagnetic order and energy spectrum in good agreement with the Heisenberg model. The case of Coulomb interaction is more complicated, but also in this case the half-filled shells agree with the Heisenberg model.

An equilateral triangle of three dots and a tetrahedron of four dots was studied in the case of partially filled *p*-shell. Also in these frustrated cases the half-filled cases are well described with the antiferromagnetic Heisenberg model while otherwise ferromagnetic coupling between the dots is favored.

In the case of lateral four dot molecules we studied the row and the square. The half-filled case is again described well with the Heisenberg model. When the interaction is the delta function repulsion the agreement is nearly perfect and for Coulomb interaction also surprisingly good. This is true for both the *p*-shell and the *sd*-shell. For other fillings the Coulomb interaction seems to favor small or zero spin for the ground state.

Acknowledgments

This work was supported by the Academy of Finland and by the Jenny and Antti Wihuri Foundation.

-
- ¹ W.A. de Heer, P. Milani, and A. Chatelain, Phys. Rev. Lett. **65**, 488 (1990)
 - ² I. M. L. Billas, A. Chatelain, and W. A. de Heer, Science **265**, 1682 (1994)
 - ³ J. P. Bucher, D. C. Douglass, and L. A. Bloomfield, Phys. Rev. Lett. **66**, 3052 (1991)
 - ⁴ D. C. Douglass, A. J. Cox, J. P. Bucher, and L. A. Bloomfield, Phys. Rev. B **47**, 12 874 (1993).
 - ⁵ S. E. Apsel, J. W. Emmert, J. Deng, and L. A. Bloomfield, Phys. Rev. Lett. **76**, 1441 (1996)
 - ⁶ J. Merikoski, J. Timonen, M. Manninen, and P. Jena, *Ferromagnetism in small clusters*, Phys. Rev. Lett. **66**, 938 (1991).
 - ⁷ G.M. Pastor, R. Hirsch, and B. Mühlischleger, Phys. Rev. Lett. **72**, 3879 (1994).
 - ⁸ F. Lopez-Urias, G.M. Pastor, Phys. Rev. B **59** 5223 (1999).
 - ⁹ M. Koskinen, M. Manninen, and S.M. Reiman, Phys. Rev. Lett. **79**, 1389 (1997).
 - ¹⁰ S.M. Reimann and M. Manninen, Rev. Mod. Phys. **74**, 1283 (2002).
 - ¹¹ R. Lopez-Sandoval, and G. M. Pastor Phys. Rev. B **67**, 035115 (2003)
 - ¹² R. Lopez-Sandoval, and G. M. Pastor Phys. Rev. B **69**, 085101 (2004)
 - ¹³ H. Lee, J.A. Johnson, M.Y. He, J.S. Speck, and P.M. Petroff Appl. Phys. Lett. **78**, 105 (2001).
 - ¹⁴ M. Schmidbauer, S. Seydmohamadi, D. Grigoriev, Z.M. Wang, Y.I. Mazur, P. Schafer, M. Hanke, R. Kohler, and G.J. Salamo, Phys. Rev. Lett. **96**, 066108 (2006).
 - ¹⁵ S. Kohmoto, H. Nakamura, S. Nishikawa, and K. Asakawa, Physica E **13**, 1131 (2002).
 - ¹⁶ H. Chen, J. Wu, Z.Q. Li, and Y. Kawazoe, Phys. Rev. B **55**, 1578 (1997).
 - ¹⁷ M. Taut, Phys. Rev. B **62**, 8126 (2000).
 - ¹⁸ C. Yannouleas and U. Landman, Int. J. Quantum Chem. **30**, 699 (2002).

- ¹⁹ S.-J. Gu, R. Fan, and H.-Q. Lin, Phys. Rev. B **76**, 125107 (2007).
- ²⁰ G. Xianlong, M. Rizzi, Marco Polini, R. Fazio, M.P. Tosi, V.L. Campo, Jr., and K. Capelle, Phys. Rev. Lett. **98**, 030404 (2007).
- ²¹ T. Koponen, J. Kinnunen, J.P. Martikainen, L.M. Jensen, P. Törmä, New. J. Phys. **8**, 179 (2006).
- ²² T.K. Koponen, T. Paananen, J.P. Martikainen, and P. Törmä, Phys. Rev. Lett. **99** 120403 (2007).
- ²³ F. Massel and V. Penna, Phys. Rev. A **72**, 053619 (2005).
- ²⁴ T. Paananen, T.K. Koponen, P. Törmä, and J.P. Martikainen *cond-mat/0801.1015*, (2008)
- ²⁵ J.K. Chin, D.E. Miller, Y. Liu, C. Stan, W. Setiawan, C. Sanner, K. Xu, and W. Ketterle, Nature **443**, 961 (2006).
- ²⁶ T. Rom, Th. Best, D. van Oosten, U. Schneider, S. Fölling, B. Paredes, and I. Bloch, Nature **444**, 733 (2006).
- ²⁷ J.-P. Nikkarila, M. Koskinen, S.M. Reimann and M. Manninen, *cond-mat/0803.2857* (2008).
- ²⁸ J. Voit, Rep. Prog. Phys. **57**, 977 (1994).
- ²⁹ E.B. Kolomeisky, and J.P. Straley, Rev. Mod. Phys. **68**, 175 (1996).
- ³⁰ E.H. Lieb and F.Y. Wu, Phys. Rev. Lett. **20**, 1445 (1968).
- ³¹ N. Yu and M. Fowler, Phys. Rev. B **45** 11795 (1992).
- ³² S. Viefers, P. Koskinen, P.S. Deo, and M. Manninen, Physica E **21**, 1 (2004).
- ³³ M. Manninen, M. Koskinen, S.M. Reimann, and B. Motelson, Eur. Phys. J. D **16**, 381 (2001).
- ³⁴ M. Koskinen, S.M. Reimann, M. Manninen, Phys. Rev. Lett. **90**, 066802 (2003).
- ³⁵ K. Karkkainen, M. Koskinen, S.M. Reimann, and M. Manninen, Phys. Rev. B **72**, 165324 (2005).
- ³⁶ K. Kärkkäinen, M. Borgh, M. Manninen, and S.M. Reimann, New J. Phys. **9**, 33 (2007).
- ³⁷ K. Kärkkäinen, M. Borgh, M. Manninen, and S.M. Reimann, Eur. Phys. J D **43**, 225 (2007).
- ³⁸ J.Kolehmainen, S.M. Reimann, M. Koskinen, and M. Manninen, Eur. Phys. J. B **13**, 731 (2000).
- ³⁹ P. Koskinen, L. Sapienza, M. Manninen, Physica Scripta **68**, 74 (2003).
- ⁴⁰ A. Harju, S. Siljamaki S, and R.M. Nieminen, Phys. Rev. Lett. **88**, 226804 (2002).
- ⁴¹ F. Mireles, S.E. Ulloa, F. Rojas, and E. Cota, Appl. Phys. Lett. **88**, 093118 (2006).
- ⁴² M. Scheibner, M. F. Doty, I. V. Ponomarev, A. S. Bracker, E. A. Stinaff, V. L. Korenev, T. L. Reinecke, and D. Gammon, Phys. Rev. B **75**, 245318 (2007).
- ⁴³ W. Zhang, T. Dong, and A.O. Govorov Phys. Rev. B **76**, 075319 (2007).
- ⁴⁴ M. Bayer, P. Hawrylak, K. Hinzer, S. Fafard, M. Korkusinski, Z.R. Wasilewski, O. Stern, A. Forchel, Science **291**, 451 (2001).
- ⁴⁵ C. Yannouleas and U. Landman, Phys. Rev. Lett. **82**, 5325 (1999).
- ⁴⁶ N.W. Ashcroft and N.D. Mermin, *Solid State Physics* (Saunders College, Philadelphia 1976).